

04

On the behavior of sodium in R7/T7 glasses under electron beam irradiation

© V.A. Kravets, T.B. Popova

Ioffe Institute,
St. Petersburg, Russia
E-mail: vladislav2033@yandex.ru

Received July 27, 2023

Revised July 27, 2023

Accepted August 1, 2023

A phenomenological description of the phenomena occurring during irradiation with an electron beam of sodium-containing glasses R7/T7 intended for the immobilization of nuclear waste is presented. The glasses were examined by the following methods: local cathodoluminescence, X-ray spectral microanalysis.

Keywords: cathodoluminescence, borosilicate glasses R7/T7, change in composition.

DOI: 10.61011/PSS.2023.10.57216.96

1. Introduction

The elemental composition and luminescent properties of sodium-containing oxide materials are extremely susceptible to electron beam irradiation. The effect of thermal diffusion of sodium from a microvolume of a sample irradiated by an electron beam is well known in X-ray spectral microanalysis [1,2]. The effect of sodium clustering in glass is known [3]. This phenomenon is explained by the field migration of mobile positive sodium ions into the region of the glass negatively charged by the electron beam.

The effect of a decrease in cathodoluminescence (CL) intensity in luminescent glasses containing sodium is also known. This CL drop in CL is associated with the formation in the sample of the defects (nonradiative recombination centers) associated with the sodium diffusion from the glass network [4,5]. The purpose of this paper is a phenomenological description of the phenomena occurring during electron beam irradiation of sodium-containing glasses R7/T7 intended for immobilization of nuclear waste [6,7]. The glasses were studied using the following methods: local cathodoluminescence, X-ray spectral microanalysis.

2. Sample

The test sample was oxide glass used for immobilization of nuclear waste „R7/T7“ with the following composition: mol%: (45.2SiO₂–17.3B₂O₃–3.9Al₂O₃–27.7Na₂O–6CaO–0.6Eu₂O₃), where ions Eu³⁺ are used as luminescent centers.

Eu³⁺, has intense luminescence in red optical band. Also Eu³⁺ can be used as a luminescent probe, which spectra is rather sensitive to structural changes of the alloyed material [8–10].

The sample was synthesized by charge melting in alumina crucible. The charge was heated to 1480°C and held for

about 60 min. in air atmosphere. The sample synthesis process is described in detail in [11].

3. Research methods

To study the elemental composition of the samples, the X-ray spectral microanalysis (EPMA) method was used. Luminescent properties were studied using local cathodoluminescence (CL) methods.

To study the samples by CL and EPMA methods, we used CAMEBAX electron probe microanalyzer (Cameca, France 1984) combined with cathodoluminescent station of an original design [12]. As CL and EPMA studies are carried out on the same device, there is possible to analyze the composition and to record CL spectra in the same region of the sample.

To ensure charge drain a carbon film was deposited onto the samples using a JEE-4C vacuum universal station (JEOL, Japan).

3.1. EPMA, X-ray spectra and sample irradiation conditions in microanalyzer

The problem was set to determine the change in the glass composition in the area of irradiation with electron probe, due to the movement of sodium atoms. We determine not absolute concentrations of elements in glass, but their changes under the influence of the electron probe. Therefore, we can limit ourselves by measurements of the intensity of analytical X-ray lines of elements, which are proportional to the mass concentrations of elements with an accuracy of „microanalyzer corrections“ [13,14]. We are interested in the movement of sodium atoms and, accordingly, in the change in its concentration in the bulk under study. But a change in the concentration of one element correspondingly leads to a change in the concentrations of all other elements. Therefore, it is possible

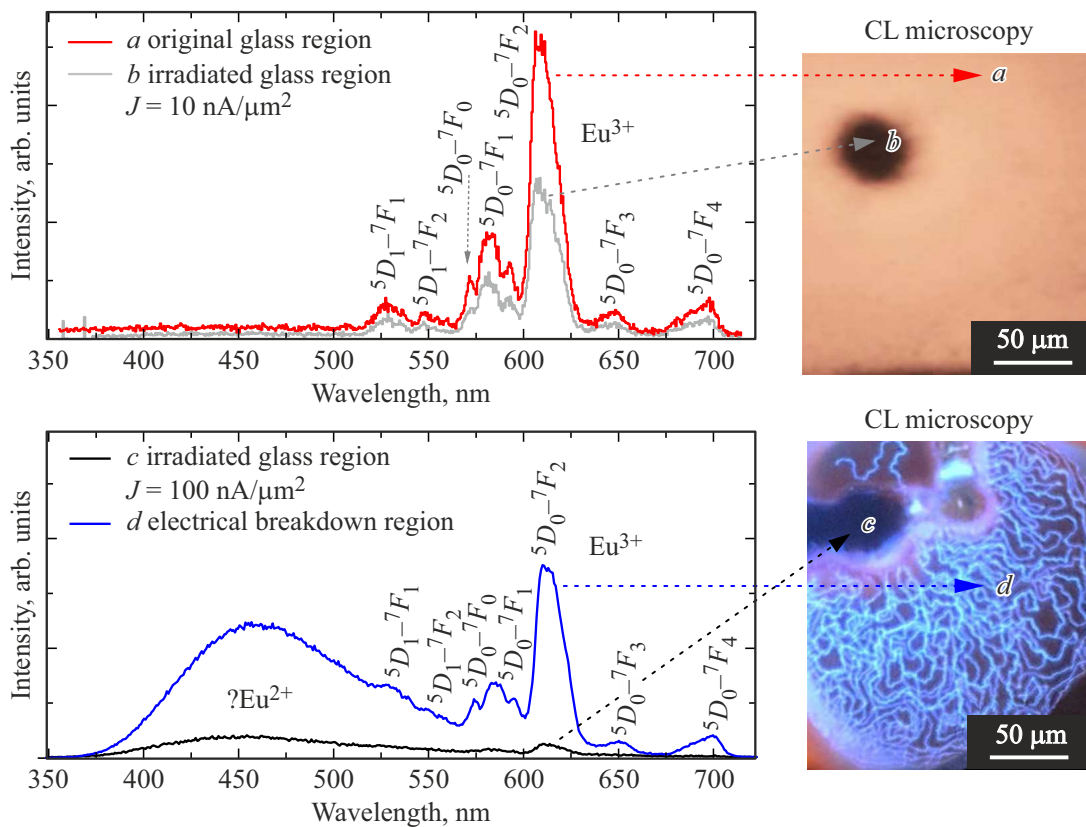


Figure 1. CL spectra obtained from sample regions with different irradiation densities: *a*) spectra of the original glass, *b*) spectra from the region irradiated at $J = 10 \text{ nA}/\mu\text{m}^2$, *c*) spectra from the region irradiated at $J = 100 \text{ nA}/\mu\text{m}^2$, *d*) spectra from the region where surface electrostatic discharges were observed.

to make conclusion about the sodium movement and the composition change under the influence of the probe by measuring the intensity of the analytical lines of other elements. In addition to measuring changes in the intensity of the Na line directly ($K\alpha$), we measured along Si line ($K\alpha$), since there is more silicon in glass than other elements and the measurement accuracy along this line is maximum.

1. Irradiation of sample with current density $J = 10 \text{ nA}/\mu\text{m}^2$.

Irradiation of the samples at an accelerating electron voltage of 15 keV with current density $J = 10 \text{ nA}/\mu\text{m}^2$ was carried out for 1 min. The electron beam radius was $5 \mu\text{m}$. The change in sample composition upon irradiation with the electron beam was studied during in situ irradiation.

2. Irradiation of sample with current density $J = 100 \text{ nA}/\mu\text{m}^2$.

Samples were irradiated with current density $J = 100 \text{ nA}/\mu\text{m}^2$ for 1 min. Change in sample composition in place of irradiation by electron beam was studied after irradiation at current density $J = 10 \text{ nA}/\mu\text{m}^2$ also for 1 min. Acceleration voltage of electrons was 15 keV. The electron beam radius was $5 \mu\text{m}$.

3.2. CL and CL-microscopy

The CL properties of the original glass and regions subjected to irradiation were studied with much lower

electron beam currents ($J = 0.1 \text{ nA}/\mu\text{m}^2$), at which no significant changes in the composition and luminescent properties of the sample occur. All CL spectra and CL images were obtained at an electron accelerating voltage of 15 keV with current density of $J = 0.1 \text{ nA}/\mu\text{m}^2$. When obtaining CL sectors, the radius of the electron beam was $5 \mu\text{m}$.

It is worth noting that the depth of penetration of the electron beam into the R7/T7 glass sample at electron accelerating voltage of 15 keV is $\sim 2 \mu\text{m}$, and the depth under the glass surface of the region of maximum energy losses of electrons is $\sim 0.5 \mu\text{m}$.

4. Results and discussion

4.1. CL and CL-microscopy

CL spectra were obtained from different regions of the irradiated glass in Figure 1 (left). The results of glass irradiation are shown in Figure 1 (right) using the CL microscopy method. Figure 1, *a* shows the CL spectrum of the original glass, before irradiation with high electron current densities. The spectrum shows transitions Eu^{3+} characteristic of borosilicate glasses [14,15].

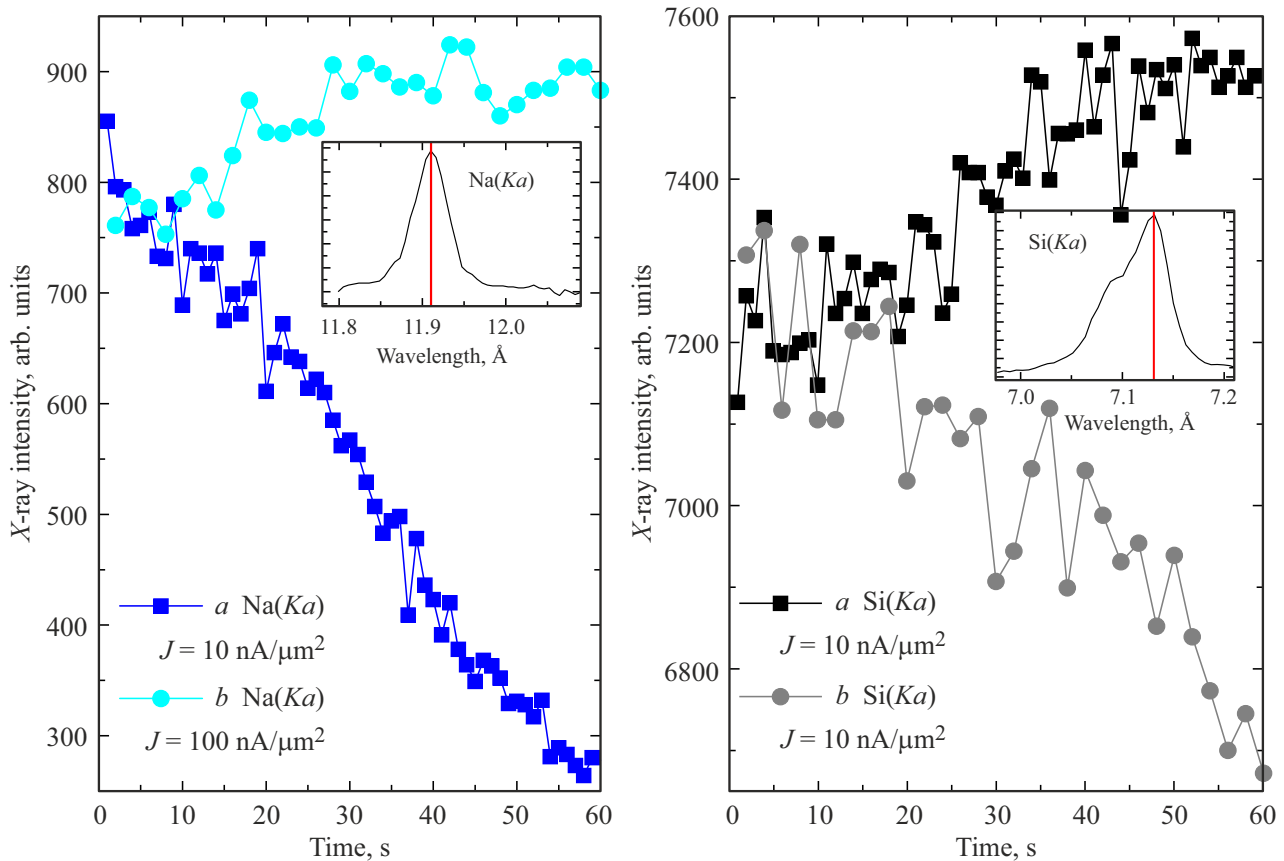


Figure 2. EPMA-study. X-ray intensity of Na($K\alpha$) (left) and Si($K\alpha$) (right) at continuous irradiation by the electron beam. *a* — for region irradiated with $J = 10 \text{ nA}/\mu\text{m}^2$, *b* — for region irradiated with $J = 100 \text{ nA}/\mu\text{m}^2$. The inserts show X-ray spectra of Na($K\alpha$) and Si($K\alpha$).

When irradiated by the electron beam with current density $J = 10 \text{ nA}/\mu\text{m}^2$ a decrease in the intensity of the CL spectrum Eu^{3+} in the irradiated region was recorded (Figure 1, *b*). A similar decrease in CL intensity (already described earlier in the introduction) is associated with the sodium diffusion from the irradiated region of the glass [4,5].

When irradiated by the electron beam with current density $J = 100 \text{ nA}/\mu\text{m}^2$ the decrease in the intensity of the CL spectrum Eu^{3+} in the irradiated region (Figure 1, *c*), surface electrostatic discharges [16] and the corresponding tracks (Figure 1, *d*) were registered. Such electrostatic discharges were not observed by the authors when irradiating glasses that did not contain alkaline components. This may indirectly indicate that Na is involved in the formation of tracks of electrostatic discharges.

At the same time, both in the irradiated region and in the region of surface electrostatic discharges a significant change in the CL color was observed in the microscope; in this region the appearance of a broad blue band in the CL spectra with a maximum in the region of 450 nm was recorded. This band has lifetimes less than 100 ns and is probably associated with change in the valence of $\text{Eu}^{3+} \rightarrow \text{Eu}^{2+}$ upon irradiation with the electron beam [17]. However, this assumption requires additional studies.

4.2. EPMA and X-ray spectra

The observed phenomena may be associated with changes in the glass composition when exposed to the electron beam. For this the dynamics of changes in the Na and Si content under continuous irradiation with the electron beam was determined. At that, the measurement of Na and Si content in the irradiated region with current density $J = 10 \text{ nA}/\mu\text{m}^2$ occurred simultaneously with irradiation. The measurement of the dynamics of Na and Si content in the irradiated region with current density $J = 100 \text{ nA}/\mu\text{m}^2$ occurred after irradiation at current density $J = 10 \text{ nA}/\mu\text{m}^2$.

The results are presented in Figure 2, *a* for the irradiated area with $J = 10 \text{ nA}/\mu\text{m}^2$ and in Figure 2, *b* for the irradiated area with $J = 100 \text{ nA}/\mu\text{m}^2$. At that Figure 2 (left) presents the dynamics of the intensity of the X-ray line Na($K\alpha$) (and, accordingly, the change in Na content in the irradiated region of the sample), and Figure 2 (right) presents the intensity of X-ray line Si($K\alpha$) (and, accordingly, the change in the Si content in the irradiated region of the sample). The sharp fluctuations in intensity are explained by the statistical nature of X-ray radiation. The inserts in Figure 2 show the actual X-ray spectra of the lines Na($K\alpha$) and Si($K\alpha$) of the sample under study.

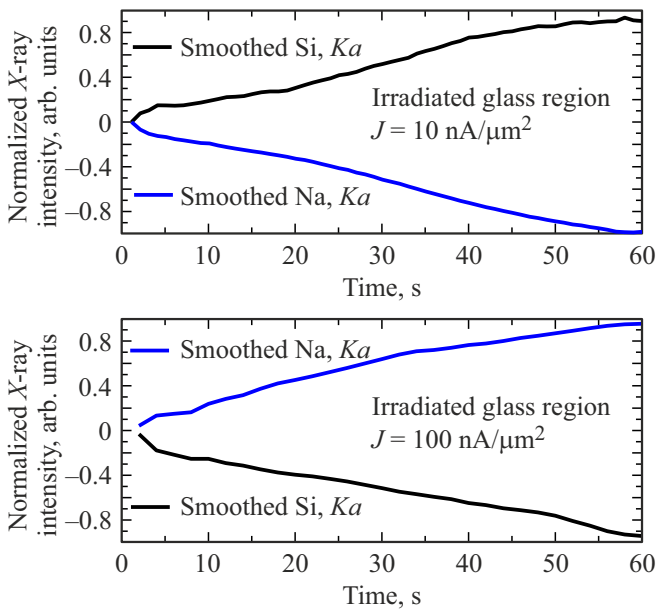


Figure 3. EPMA-study. Smoothed and normalized X-ray-intensities of Na($K\alpha$) and Si($K\alpha$) under continuous irradiation with the electron beam. On top: for region irradiated with $J = 10 \text{ nA}/\mu\text{m}^2$. In bottom: for region irradiated with $J = 100 \text{ nA}/\mu\text{m}^2$.

For the region irradiated with $J = 10 \text{ nA}/\mu\text{m}^2$ the decrease in Na content is observed. This effect is explained by the thermal diffusion of sodium from the irradiated region of the glass [1,2].

For the region irradiated with $J = 100 \text{ nA}/\mu\text{m}^2$ the increase in Na content is observed. This effect can be explained by the formation of a sodium-depleted region of the glass (irradiated region) due to sodium clustering [3,18]. The depletion of sodium in the irradiated area occurs due to the sodium migration from the network structure of glass into clusters, which creates a concentration gradient between the irradiated and non-irradiated regions of the glass. This results in the observed sodium movement into the irradiated region due to the concentration gradient.

If we assume that irradiation with the electron beam leads to changes in the sodium content, then the change in Si content in glass with change in the mass content of Na has the form

$$-\Delta\text{Si} = \Delta\text{Na} \cdot M_{\text{Si}} / \sum M_{\text{All-Na}},$$

where ΔSi — change in the mass concentration of Si in the material, ΔNa — change in the mass concentration of Na in the material, M_{Si} — mass concentration of silicon in the material and $\sum M_{\text{All-Na}}$ — sum of mass concentrations of all elements in the material, without (minus) Na. In this case, the value $M_{\text{Si}} / \sum M_{\text{All-Na}}$ is constant when the Na content changes.

Thus, changes in the Si content should, with accuracy to a constant, symmetrically repeat changes in the Na content in the material: $-\Delta\text{Si} \sim \Delta\text{Na}$.

Figure 3 demonstrates normalized and smoothed (processed) curves of the intensity change of the X-ray lines Na($K\alpha$) and Si($K\alpha$) under continuous irradiation with an electron beam.

Taking into account errors the changes in the concentrations of Si and Na in the material are symmetrical relative to each other $-\Delta\text{Si} \sim \Delta\text{Na}$. Thus, it can be stated that the observed change in the Si concentration in the irradiated material occurs due to either Na thermal diffusion or Na clustering in the irradiated region of the material.

This indirectly confirms the fact that changes in composition occur in glass only due to Na; if there were changes in the content of other elements, then the curves in Figure 3 would not be symmetrical.

5. Conclusion

When irradiated with the electron beam the decrease in the intensity of CL spectrum Eu^{3+} in the irradiated region, surface electrostatic discharges and their corresponding tracks were registered. The significant change in composition was observed in the region exposed to prolonged electron beam irradiation. Processes associated with both the sodium thermal diffusion from the irradiated area and processes associated with the sodium clustering in glass were recorded. At that, in the region irradiated with electron current density $J = 10 \text{ nA}/\mu\text{m}^2$ processes of Na thermal diffusion prevail, and in the region irradiated with electron current density $J = 100 \text{ nA}/\mu\text{m}^2$ Na clustering processes prevail. Thus, it was shown that the composition of glasses of R7/T7 series is not stable when exposed to the electron beam. This is reason of doubts about the feasibility of this glass use for radioactive materials processing.

Acknowledgments

The authors express their gratitude to the staff of the Laboratory of „Diffusion and Defect Formation in Semiconductors“ of Ioffe Physicotechnical Institute.

Conflict of interest

The authors declare that they have no conflict of interest.

References

- [1] D.M. Usher. *C14*, 2039 (1981).
- [2] H. Bach. *Rad. Effects* **28**, 215 (1976).
- [3] E.S. Bochkareva, N.V. Nikonorov, O.A. Podsvirov, M.A. Prosnikov, A.I. Sidorov. *Plasmonics* **11**, 241 (2016).
- [4] M. Kayama, H. Nishido, M. Lee, K. Ninagawa. *Am. Mineralogist* **99**, 1, 65 (2014).
- [5] N. Ollier, B. Boizot, P. L'henoret, S. Guillous, G. Petite. *J. Appl. Phys.* **11** (2009).
- [6] M.I. Ojovan, W.E. Lee, S.N. Kalmykov. Elsevier, Amsterdam, The Netherlands (2005). 497 p.

- [7] P. Frugier, S. Gin, L.D. Windt, G. Santarini. *J. Nucl. Mater.* **380**, 1, 8 (2008).
- [8] E.V. Ivanova, V.A. Kravets, K.N. Orekhova, G.A. Gusev, T.B. Popova, M.A. Yagovkina, O.G. Bogdanova, B.E. Burakov, M.V. Zamoryanskaya. *J. Alloys Compd.* 808 (2019).
- [9] V. Kravets, E.V. Ivanova, M.I. Moskvichev, M. Zamoryanskaya. *Opt. Spectroscopy* **129**, 2, 245 (2021).
- [10] G.A. Gusev, S.M. Masloboeva, V. Kravets, M.A. Yagovkina. *Inorganic Mater.* **57**, 4, 383 (2021).
- [11] V. Kravets, E.V. Ivanova, A.N. Trofimov, M. Zamoryanskaya. *J. Lumin.* **226**, 117419 (2020).
- [12] M.V. Zamoryanskaya, S.G. Konnikov, A.N. Zamoryanskii. *Instrum. Exp. Tech.* **47**, 4, 477 (2004).
- [13] S.J.B. Reed. *Electron microprobe analysis and scanning electron microscopy in geology.* Cambridge University Press (2005).
- [14] L. Reimer. *Measurement Sci. Technol.* **11**, 12, 1826 (2000).
- [15] H. Lin, D. Yang, G. Liu, T. Ma, B. Zhai, Q. An, J. Yu, X. Wang, X. Liu, E. Yue-Bun Pun. *J. Lumin.* **113** (2005).
- [16] R.H. Khasanshin, L. Novikov, S.B. Korovin. *J. Surface Investigation-x-ray Synchrotron Neutron Techniques* **9**, 1, 81 (2015).
- [17] H. Ebendorff-Heidepriem, D. Ehrt. *Phys. Chem. Glasses-Eur. J. Glass Sci. Technol. B* **61**, 5, 189(2020).
- [18] Z.O. Lipatova, E. Kolobkova, A.I. Sidorov, N. Nikonorov. *Opt. Spectroscopy* **121**, 2, 200 (2016).

Translated by I.Mazurov